DNA self-assembly-driven positioning of molecular components on nanopatterned surfaces

M Szymonik, A G Davies and C Wälti

School of Electronic and Electrical Engineering, University of Leeds, Leeds LS2 9JT, UK

E-mail: c.walti@leeds.ac.uk

CrossMark

Abstract

We present a method for the specific, spatially targeted attachment of DNA molecules to lithographically patterned gold surfaces—demonstrated by bridging DNA strands across nanogap electrode structures. An alkanethiol self-assembled monolayer was employed as a molecular resist, which could be selectively removed via electrochemical desorption, allowing the binding of thiolated DNA anchoring oligonucleotides to each electrode. After introducing a bridging DNA molecule with single-stranded ends complementary to the electrode-tethered anchoring oligonucleotides, the positioning of the DNA molecule across the electrode gap, driven by self-assembly, occurred autonomously. This demonstrates control of molecule positioning with resolution limited only by the underlying patterned structure, does not require any alignment, is carried out entirely under biologically compatible conditions, and is scalable.

S Online supplementary data available from stacks.iop.org/NANO/27/395301/mmedia

Keywords: DNA nanotechnology, self-assembly, hybrid molecular electronic devices

(Some figures may appear in colour only in the online journal)

1. Introduction

One of the key challenges in molecular nanotechnology lies in interfacing nanoscale structures with solid-state devices. Molecular constructs of increasingly complex structure and functionality are being developed, but connecting them together into higher-order assemblies, interfacing them with larger microelectronic devices at multiple points in a controllable and scalable fashion, and ensuring that these delicate molecular structures are not damaged in the process of being bound to solid supports, all remain problematic.

The usual approach for attaching biological molecules to a surface consists of coating the surface with a biocompatible layer—such as a polymer matrix, gel, or self-assembled monolayer (SAM)—that contains anchoring or attachment groups which can subsequently bind larger molecular assemblies [1]. The attachment points can be reactive chemical groups or small biological molecules with specific binding capabilities, such as DNA. To enable specific and directed multi-point interfacing of molecular assemblies, different attachment points with distinct binding properties have to be established on the microelectronic device. The selective self-assembly and molecular recognition properties inherent to DNA make it an ideal candidate for multi-point molecular attachment applications—a schematic illustration of this concept is shown in figure 1.

DNA is a particularly versatile molecular engineering tool [2, 3], enabling rational *ab initio* design of DNA-based structures and devices [4]. Double-stranded DNA (dsDNA) is a robust molecule comprising two reverse complementary single-stranded DNA (ssDNA) molecules assembled into a double-helical structure. The ssDNA molecules, which are simple linear polymers, provide exquisitely specific molecular recognition properties and so make an attractive material for use as a molecular anchor. Short fragments of ssDNA are
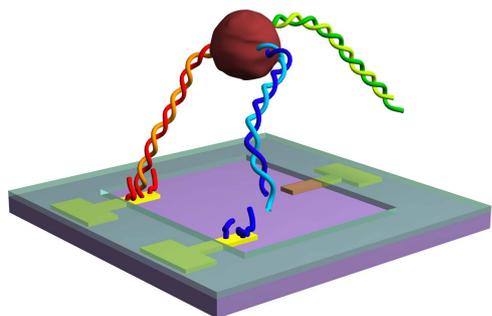
Figure 1. Proposed molecular patterning scheme in which different domains of a molecular construct can be bound onto appropriately functionalised electrodes via DNA self-assembly.

economical to synthesise, and multiple approaches exist for attaching ssDNA to other nanoscale materials.

In general, ssDNA is first modified with an appropriate functional chemical group—usually a thiol or amine moiety—to provide covalent attachment to a solid surface. Once attached, the ssDNA can then act as a molecular anchor and bind complementary oligonucleotides [5–7] and larger structures [8–10]. However, it is challenging to bind the DNA anchors with spatial precision on a surface, especially on a sub-micron scale. Deposition techniques include nanopipetting [11], dip-pen lithography [12] and micro-contact printing [13, 14], but all have significant drawbacks, including limited resolution, poor scalability, and difficulty of alignment with existing features. Previously, however, we developed an alternative technique for the selective deposition of different biomolecules onto closely-spaced gold electrodes, demonstrating patterning at a sub-50 nm resolution [15]. An electrode array is first coated with an alkanethiol SAM that acts as a molecular resist, preventing attachment of anchor molecules. Applying a negative bias to selected electrodes desorbs the SAM locally [16], allowing attachment of biomolecules onto the electrodes that are exposed. This can be repeated sequentially to pattern different DNA anchors across the surface. This technique has been demonstrated for monolayer patterning [17], DNA [15, 18] and peptide binding [19] as well as cell capture and release [20], and potentially allows the wiring of individual molecular constructs in a site-directed fashion.

In this paper, we demonstrate the ability of this approach to direct the assembly of single-molecule constructs. We selectively functionalised pairs of nanopatterned electrodes separated by less than 100 nm with DNA oligonucleotides, providing specific and distinct binding points to enable the self-assembly of a bridging DNA molecule across the gap between the electrodes. Previous investigations in which DNA is spanned across a gap between two electrodes have either deposited the DNA non-specifically [21, 22], attached the DNA to only one side of the gap [23], attached the DNA to both electrodes using the same linker chemistry [24], or coated both electrodes with the same DNA sequence, followed by introduction of a strand with two identical complementary ends [12, 25]. The use of two discrete DNA sequences as attachment points has been demonstrated in which the DNA oligonucleotides were deposited onto 10 μm-

separated electrodes by a nano-pipette [9], and molecular combing used to stretch the bridging fragment between the electrodes. Roy *et al* [26] used an electrochemical desorption approach similar to ours to coat two vertically stacked electrodes selectively, followed by bridging and metallisation. However, the vertical configuration limits the applicability of this approach for directed self-assembly applications—the number and location of possible binding events was only observed indirectly and not finely controlled.

2. Results and discussion

2.1. Optimisation of surface preparation conditions for selective DNA binding

The use of thiol end-modification has been shown to be a flexible and convenient way of covalently tethering short DNA oligonucleotides to gold surfaces [5, 6]. Typically, gold surfaces are incubated in aqueous solutions of the DNA oligonucleotide to form a monolayer of DNA on the surface. While densities of the order of 10^{12}–10^{13} molecules per cm^2 can be obtained [27], the resulting monolayers still contain large numbers of defects. Therefore, after DNA incubation, a short alkanethiol molecule is normally used to backfill the surface, filling the gaps between the ssDNA molecules and displacing any non-specifically bound DNA, i.e. DNA oligonucleotides adsorbed onto the surface via interactions other than the covalent gold–thiol bond. Furthermore, this assists the DNA to protrude into the solution, allowing efficient hybridisation with complementary DNA oligonucleotides [5–7].

The molecular lithography technique used in this work exploits the use of an alkanethiol SAM as a molecular resist in order to block and expose electrodes specifically for DNA binding. The blocked surface needs to prevent both specific and non-specific adsorption of DNA, whereas the un-blocked surface must allow efficient binding of thiolated DNA but ought to minimise non-specific binding. The DNA must bind such that subsequent hybridisation of complementary DNA occurs with high efficiency. Finally, following DNA functionalisation and backfilling, the surface must prevent further binding, like the blocked, non-functionalised surface.

We employed a colorimetric method analogous to western blotting to determine the optimal reaction conditions for attaching DNA onto gold surfaces, and its subsequent hybridisation [28]. In brief, a gold surface was spotted with droplets of thiolated DNA molecules, followed by spotting with biotin-modified complementary DNA. The thiol-functionalised probe oligonucleotide A was 20 bases, with a 3′ thiol, attached via a 3 carbon linker, while oligo B was 24 bases, with a 5′ thiol and 6 carbon linker. An enzymatic staining step targeting the biotin produces a local colour stain where ssDNA attachment and subsequent hybridisation has occurred.

In comparison with commonly used 1-mercapto-6-hexanol [5–7] and a number of other alternative blocking layers, 1-mercapto-11-undecanol (HS(CH$_2$)$_{11}$OH, MCU) was found to produce significantly lower levels of non-specific binding
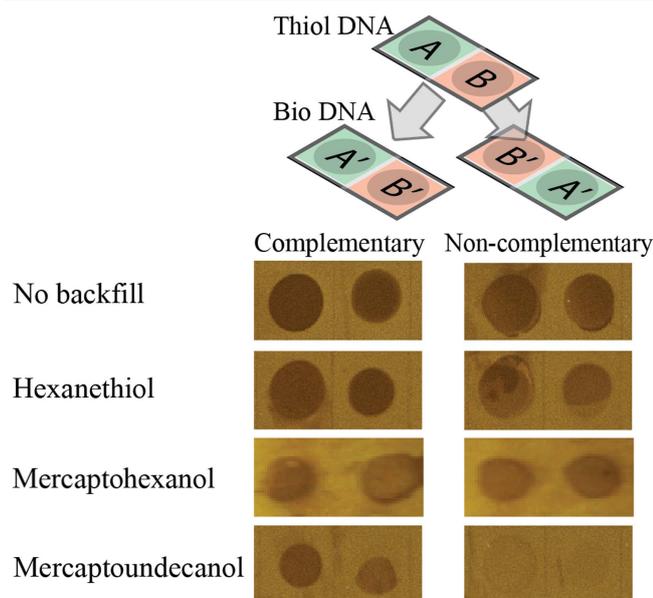
Figure 2. Colorimetric staining obtained when surface-bound thiolated DNA oligonucleotides were backfilled with SAM molecules and exposed to complementary and non-complementary biotinylated DNA. The effectiveness of various backfilling molecules is shown. The left side of each panel was incubated with DNA anchor A; the right side was incubated with DNA anchor B.

and better blocking performance (figure 2). Longer chain alkanethiols are expected to form better-packed monolayers [29] and the advantages of their use as backfilling molecules have been reported [30, 31]. The efficacy of the blocking layers correlates well with indicators of the SAM quality, such as the water contact angle and electrochemical blocking of redox reactions at the surface (data not shown), but the characteristics of the exposed head groups were also found to be of importance. For example, hexadecanethiol $(HS(CH_2)15CH_3)$ forms high-quality monolayers but the hydrophobic head group leads to non-specific binding, likely caused by aggregation of DNA and other biological molecules.

As a further refinement, the thiolated DNA was co-adsorbed with MCU present in the incubation solution, in addition to the MCU backfilling step. Such a co-adsorption approach has previously been reported to provide good control over the surface probe density and monolayer quality [31–33]. Figure 3(a) shows the typical incubation, hybridisation and staining scheme. Four spots on the gold surface were functionalised with thiolated DNA by co-adsorbing the DNA with MCU before the surface was backfilled with MCU. A second functionalization step was then carried out where thiolated DNA of a different sequence was applied to the four spots, before each spot was challenged with biotinylated DNA. The presence of the DNA-bound biotin was then detected using the staining protocol.

As shown in figure 3(b), in the absence of MCU, some surface staining was present even where the target probe was introduced after the surface is nominally blocked. Increasing the amount of MCU in the first DNA incubation solution,

while keeping DNA concentration constant, reduced this undesirable binding. Addition of excess MCU eventually led to a complete lack of staining. DNA:MCU ratios above 1:10 and below 1:100 were found to yield strong staining—in agreement with reports on similar systems in the literature [34, 35]—while reliably preventing the adsorption of DNA via non-specific interactions. Hence, a 1:50 DNA:MCU ratio was employed for all subsequent experiments. This was found to be a robust approach to generate the desired surface properties—making surface-tethered ssDNA probes available for hybridisation with complementary DNA while resisting the non-specific adsorption of other DNA molecules.

2.2. Molecular lithography via desorption of alkanethiol SAMs

The optimised surface attachment protocol was used together with electrochemical desorption to functionalise sequentially opposing pairs of nanogap electrodes with different ssDNA molecules. The functionalization scheme is presented in figure 4(a). The entire surface was first blocked with an MCU layer. This blocking layer was then electrochemically desorbed from a first set of electrodes by applying a negative voltage to break the gold–thiol bond [16]. This resulted in a clean gold surface, which readily binds thiol-functionalised DNA. Thiolated DNA anchor A was then bound onto the exposed electrodes and the surface backfilled with MCU. A second set of electrodes was then electrochemically desorbed and functionalised with thiolated DNA anchor B. Figure 4(b) shows the colorimetric staining for two devices functionalised this way and subsequently challenged with biotinylated DNA complementary to either DNA anchor A or B. The localised dark staining indicates the successful patterning of neighbouring nanogap electrodes with the two DNA sequences.

Here, the thiolated DNA and MCU were present in the electrochemical buffer during desorption at a ratio of DNA:MCU of 1:50, rather than being applied to the surface afterwards as in previous work [15]. This sped up the process and was found to improve the uniformity of the thiol-DNA binding, especially around electrode edges—an issue possibly caused by re-adsorption of the sparsely soluble MCU onto the electrode surface.

This technique thus enables selective molecular patterning of features at sub-micron scale. The electrochemical patterning approach brings several key advantages. The process is carried out under aqueous, near-physiological conditions. Importantly, the biomolecule pattern is entirely self-aligning to the underlying metal features and its resolution is theoretically limited only by the dimensions of this gold pattern. The process is also, in principle, scalable and should allow for the parallel functionalization of many electrodes with the same biomolecule as well as the serial pattering of many distinct molecules.

2.3. Bridging of nanogap electrodes

In order to self-assemble a dsDNA molecule across the gap between two opposing electrodes functionalised with different DNA anchors, the double-stranded molecule requires two single-stranded overhangs, each complementary to one of the

a) Spotting pattern:

b) Staining produced and quantified intensity:
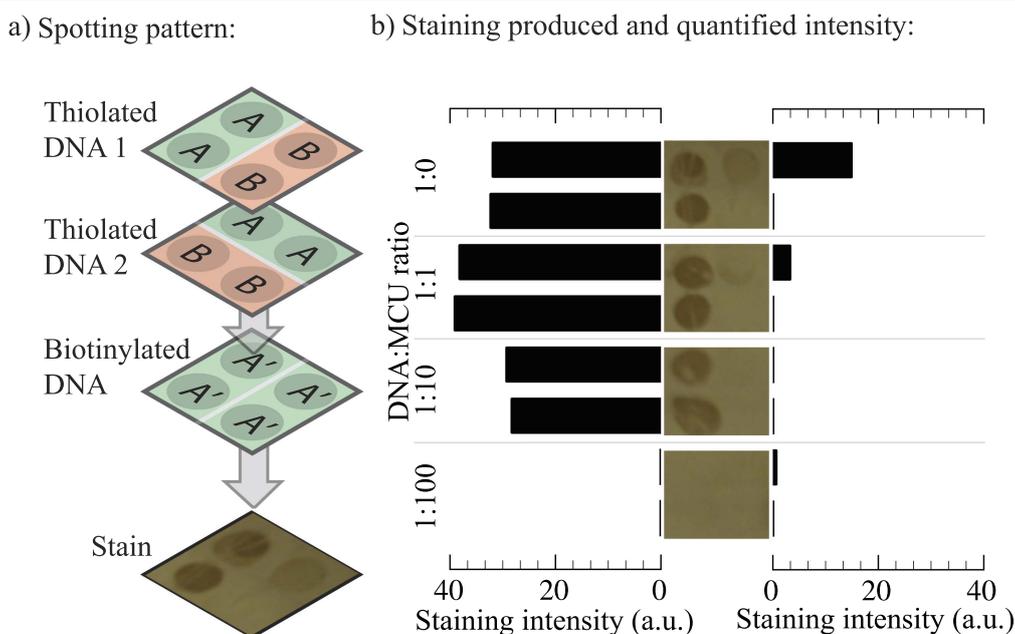
Figure 3. (a) DNA incubation, hybridisation and detection with two thiol-DNA incubation steps, testing the ability of the surface to resist further thiol-DNA binding onto the surface after an initial incubation and MCU backfill. (b) Colorimetric staining obtained for different concentrations of MCU in the incubation solution. The bars represent the quantified staining intensity of the corresponding spots.

DNA anchors. The double-stranded bridging DNA was designed to include two nicking restriction sites which allow a single strand of the dsDNA to be cut at an appropriate location. The 330 base-pair DNA molecules were generated by PCR amplification of a short fragment from λ-bacteriophage DNA, then digested with the nicking enzyme Nt.BstNBI and purified to yield single-stranded overhangs complementary to the probe strands A and B. Details of the DNA synthesis are described in the supplementary information (stacks.iop.org/NANO/27/395301/mmedia).

Nanogap electrode arrays, where opposing electrodes were functionalised with DNA anchor A and B, were then exposed to a solution containing the bridging DNA, and incubated for 4 h. After incubation, features clearly resembling dsDNA molecules spanning the nanogap were identified via AFM imaging, as shown in figure 5. The dimensions of the bridging features were consistent with those of DNA strands freely deposited on silicon oxide surfaces. No such bridging events were seen across any of the non-functionalized electrodes. The nanogaps shown appear to be bridged by one, two and 3–4 DNA strands, as indicated by height profiles across the gaps (figure 5).

Colorimetric staining showed that biotin-functionalised DNA constructs analogous to the bridging strand bind specifically to the surface probe with little non-specific background (see supplementary information, figure S2). To confirm further that the bridging material was specifically assembled, the DNA anchor on one of the electrodes was removed by electrochemical desorption. As a result, the DNA molecule spanning the gap disappeared, suggesting that binding is indeed occurring via hybridisation to the gold–thiol bonded DNA anchors, rather than by non-specific adsorption (see supplementary information, figures S3 and S4).

The specific and programmable attachment of large biological molecules and nanoscale constructs to surfaces is challenging due, in large parts, to their multitude of possible interactions with the surface and other molecules in the mixture. While the gold–thiol bond is stronger than any non-specific interactions of individual DNA bases with gold [36], as the length of the DNA polymer grows the combined non-specific interactions dominate the behaviour of the system [7]. Here, we have used thiol–gold chemistry to introduce short, well-behaved anchor points that then allow the self-assembly-driven attachment of larger structures. The optimised surface design combined with stringent washing helped minimise non-specific binding, while the DNA anchors provided strong and highly specific binding targets at the desired locations.

3. Conclusions

We have demonstrated a DNA-self-assembly-based approach which enables the positioning of single biological molecules onto solid-state devices with nanoscale resolution. Short DNA fragments are attached to the surface first, which then act as anchor sites for the larger structure. The short DNA strands can be bound to the surface in a controlled fashion [30], while providing a stable and highly specific anchor point for subsequent attachment of the larger DNA molecule by self-assembly. The approach allows the multi-point attachment of single biomolecules. The strength, flexibility and density of the attachment points can be adjusted by varying the DNA anchor sequence and immobilisation reaction conditions. The mixed DNA oligonucleotide–alkanethiol layer employed here can be engineered to resist non-specific

a)

Clean gold electrode array

Assemble blocking MCU SAM

Desorb electrodes

Incubate thiol oligo A, backfill

Desorb opposing electrodes

Incubate thiol oligo B, backfill

b) Hybridisation with biotinylated complement and colorimetric detection:

5X

50X

c) DNA bridging:
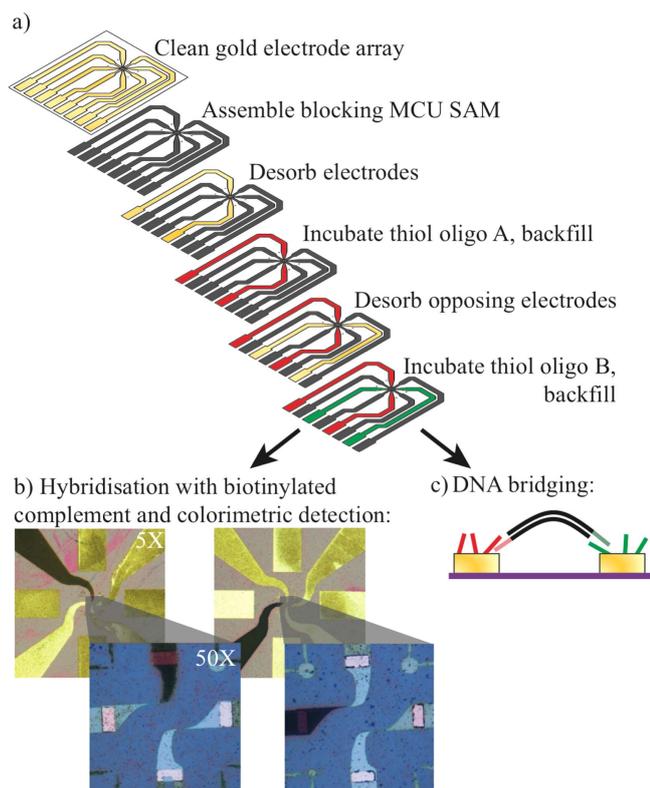
Figure 4. (a) Schematic diagram showing the sequence of incubation steps employed to bind selectively two distinct DNA anchors to chosen electrodes on a device. (b) Optical microscope images showing the central areas of two electrode array devices each featuring two sets of opposing electrodes separated by approximately 50 nm. The devices were both functionalized in the same way, as shown in (a), but each was challenged with biotinylated DNA complementary to the DNA bound on one side of the nanogap (oligo A′ or B′, respectively) followed by colorimetric visualisation of the biotin. (c) Schematic illustration showing the attachment of a bridging DNA strand to the functionalised electrodes.

adsorption of relevant molecules, and the stability of this surface layer means that strong washing and denaturing treatments can be used—the stringency of the surface treatment can be tuned to the specific molecular assembly.

The electrochemical desorption of alkanethiol blocking layers is a powerful molecular lithography technique. The blocking SAM is specifically formed on and removed from the entirety of the target electrode, meaning no alignment is needed and the resolution is theoretically limited only by the size of the underlying pattern. No additional design considerations or device processing are necessary beside the need for an electrical contact. Fabrication and electrical addressing of large numbers of metal electrodes are readily achievable and modern microfluidics enable the automation of surface functionalization, thus making this approach parallelisable and scalable. Furthermore, the molecular lithography steps—monolayer formation, removal and attachment of surface anchors—can be carried out under physiological conditions, enabling the exploitation of a large range of biological interactions to drive the surface assembly.

Our technique offers a convenient method for the rational self-assembly of nanoscale constructs and overcomes several

key limitations present in alternative approaches. More complex molecular constructs could be positioned by introducing additional anchor points on suitably placed neighbouring electrodes. As such, the technique has the potential to be a powerful tool for the controlled assembly of nanoscale hybrid molecular and electronic devices.

4. Methods

4.1. Nanogap lithography

The electrode fabrication was carried out in two steps. First, the large interconnects were defined via optical lithography using a bilayer resist process. A 5% solution of 495 kDa polymethyl methacrylate (PMMA) in anisole was spun on the Si/SiO_2 wafers at 4000 RPM, followed by a 1 h bake at 170 °C. Subsequently, Microposit S1805 photoresist (MicroChem, USA) was spun onto the wafers at 5000 RPM followed by a 1 min bake at 115 °C. The devices were then UV exposed through a quartz mask with a dose of 20 mJ cm^{-2} on a Karl Suss MJB3 mask aligner, developed in Microposit MF319 developer for 40 s, and water rinsed. After blow-drying, the underlying PMMA layer was exposed to UV-ozone irradiation for 15 min (Jelight, USA). The samples were then developed in a 1:3 methyl isobutyl ketone isopropanol (MIBK:IPA) solution for 20 s followed by a dip in IPA. An electron beam evaporator was used to deposit 2 nm of chrome and 30 nm of gold. After lift-off, the samples were again cleaned in acetone and IPA, coated with two layers of a PMMA resist—3% 495 kDa spun at 3000 RPM, followed by 2% 950 kDa PMMA spun at 5000 RPM, both followed by a 1 h bake at 170 °C—and the nanogap electrodes were then defined via electron-beam lithography using a Leo–Raith tungsten filament system. The nanogap size was controlled by varying the dose between ~500–700 μC cm^{-2} at 30 kV. The samples were developed in MIBK:IPA for 70 s and another chrome/gold evaporation was carried out as above. The quality of patterning was verified using the electron-beam lithography system in imaging mode as well as by tapping mode AFM using a Dimension 3100 (Veeco, USA) and OTESPA tips (Bruker, USA). Optical images of a typical device are shown in figure 6.

4.2. Colorimetric detection of DNA binding and hybridisation

Freshly evaporated and cleaned gold surfaces were spotted with a solution of 5 μM thiolated DNA oligonucleotide, 250 μM 1-mercapto-11-undecanol (97%, Sigma-Aldrich, UK; MCU) and 1 M NaCl in pH8 tris-EDTA (TE) buffer. 1 μl spots of this solution were pipetted onto the gold surface and incubated in a humid chamber for 1 h. The samples were then washed in TE buffer, and backfilled by immersion in a freshly sonicated 1 mM aqueous solution of MCU. After 1 h, the samples were rinsed with water and blow-dried. Hybridisation was carried out by spotting 1 μl of 5 μM DNA in 1 M NaCl in TE onto the DNA-functionalised areas on the gold surface. Samples were incubated for 1.5 h, followed by a triple wash in TE. The surfaces were then blocked from non-specific
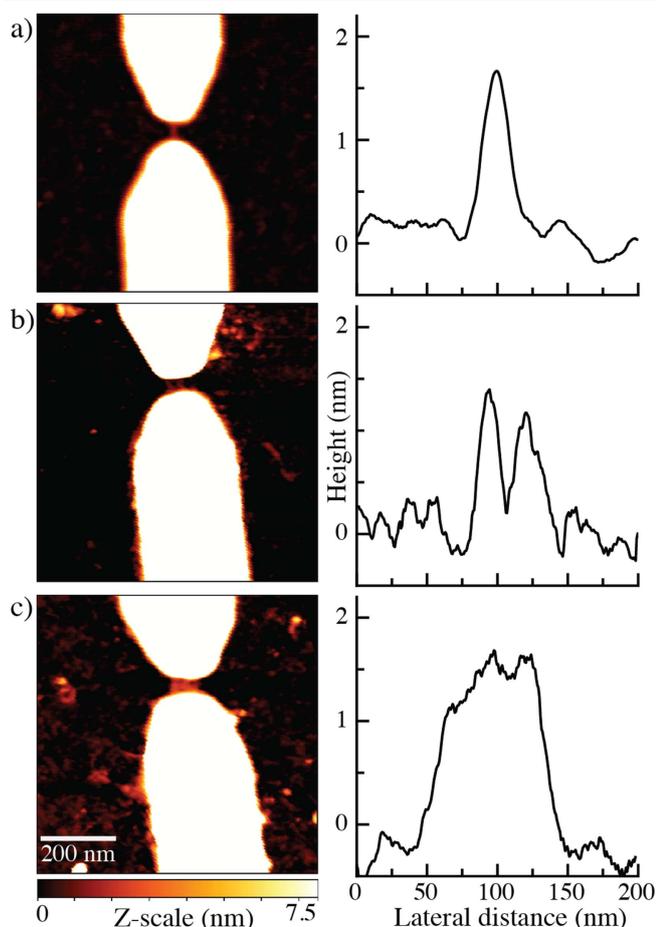
Figure 5. Nanogap electrode devices after bridging with the 330 base pair DNA construct. AFM images (left) and height profiles along lines bisecting each gap (right) are shown for devices that appear to have bound one (a), two (b), and multiple (c) DNA strands. Figure S3 in the supplementary information shows the same images with an extended Z-scale.

protein adsorption by incubating in 1% bovine serum albumin in tris-buffered saline (50 mM tris-HCl, 150 mM NaCl, pH 7.4; TBS) for 2 h. After a gentle rinse in TBS, the samples were exposed to a 1:1000 solution of anti-biotin antibody conjugated with alkaline phosphatase (Sigma-Aldrich, Germany; anti-biotin:AP) in TBS with 0.05% Tween-20 (TBS-Tween) for 45 min. This was followed by thorough rinsing, with four 5 min washes in TBS-Tween and three washes in TBS. The sample was then developed by immersion in a freshly prepared solution of SigmaFast BCIP/NBT (Sigma-Aldrich, UK) for 20 min in a light-sealed box. Finally, the samples were dipped in ultrapure-water (18.2 MΩ cm, Millipore, UK) and blow dried, before imaging with either a digital camera or Zeiss Axio Scope microscope. All other monolayer precursors tested were purchased from Sigma-Aldrich (UK).

4.3. DNA anchor attachment to surface and bridging DNA assembly

Prior to functionalization, the patterned electrode surfaces were cleaned by ultrasonic agitation in acetone followed by
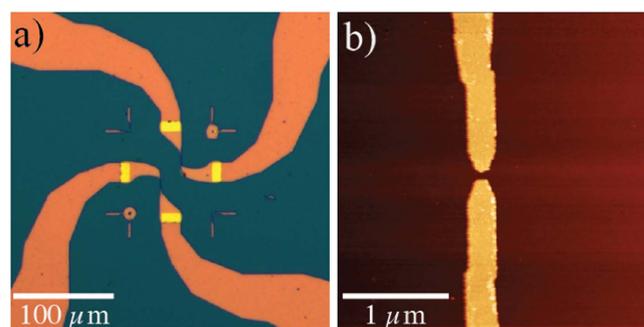
Figure 6. (a) Optical image of a patterned device. (b) AFM micrograph of a typical nanogap feature on the device.

isopropanol for 10 min each, a 20 min UV-Ozone treatment, and 20 min of sonication in ethanol. The gold surfaces were then immersed overnight in a 1 mM solution of MCU in ethanol. DNA electrochemical deposition was carried out directly in solutions containing the thiolated DNA oligomers to be bound to the surface, in a custom-built 80 μl cell, with a platinum wire counter and miniature Ag/AgCl reference electrodes. The solutions comprised 5 μM DNA, 250 μM MCU, and 1 M NaCl, in pH 11 100 mM sodium phosphate buffer. Owing to the low solubility of MCU in water, its aqueous solutions were prepared by sonication immediately before use. The electrochemical potential of the electrodes to be functionalized was cycled between −0.5 and −1.5 V versus Ag/AgCl five times at 100 mV s^{-1} and then held at −1.5 V for 1 min, while all other electrodes were held at 0 V. The samples were then incubated for 10 min, washed repeatedly in TE buffer and immersed in a 1 mM aqueous solution of MCU for 1 h. This was repeated for other electrodes as appropriate with different thiolated DNA oligonucleotides. To verify the binding of the thiolated DNA molecules, the colorimetric protocol described above was used.

After patterning of electrodes with the desired DNA oligonucleotide sequences, the electrode arrays were spotted with 2 μl of the bridging DNA at 65 ng μl^{-1} in pH 8 TE buffer with 1 M NaCl. After 4 h of incubation, the electrodes were rinsed with TE buffer and washed three times for 5 min The samples were then blow dried with N$_2$ and imaged via tapping mode AFM.

References

[1] Jonkheijm P, Weinrich D, Schröder H, Niemeyer C M and Waldmann H 2008 Chemical strategies for generating protein biochips *Angew. Chem., Int. Ed. Engl.* **47** 9618–47

[2] Seeman N C 2010 Nanomaterials based on DNA *Annu. Rev. Biochem.* **79** 65–87

[3] Pinheiro A V, Han D, Shih W M and Yan H 2011 Challenges and opportunities for structural DNA nanotechnology *Nat. Nanotechnol.* **6** 763–72

[4] Douglas S M, Marblestone A H, Teerapittayanon S, Vazquez A, Church G M and Shih W M 2009 Rapid prototyping of 3D DNA-origami shapes with caDNAno *Nucleic Acids Res.* **37** 5001–6

[5] Peterlinz K, Georgiadis R, Herne T and Tarlov M 1997 Observation of hybridization and dehybridization of thiol-tethered DNA using two-color surface plasmon resonance spectroscopy *J. Am. Chem. Soc.* **119** 3401–2

[6] Steel A, Herne T and Tarlov M 1998 Electrochemical quantitation of DNA immobilized on gold *Anal. Chem.* **70** 4670–7

[7] Steel A B, Levicky R L, Herne T M and Tarlov M J 2000 Immobilization of nucleic acids at solid surfaces: effect of oligonucleotide length on layer assembly *Biophys. J.* **79** 975–81

[8] Schreiner S M, Hatch A L, Shudy D F, Howard D R, Howell C, Zhao J, Koelsch P, Zharnikov M, Petrovykh D Y and Opdahl A 2011 Impact of DNA–surface interactions on the stability of DNA hybrids *Chem. Rev.* **83** 4288–95

[9] Braun E, Eichen Y, Sivan U and Ben-Yoseph G 1998 DNA-templated assembly and electrode attachment of a conducting silver wire *Nature* **391** 775–8

[10] Walter A, Wu J, Flechsig G-U, Haake D A and Wang J 2011 Redox cycling amplified electrochemical detection of DNA hybridization: application to pathogen *E. coli* bacterial RNA *Anal. Chim. Acta* **689** 29–33

[11] Bruckbauer A, Ying L, Rothery A M, Zhou D, Shevchuk A I, Abell C, Korchev Y E and Klenerman D 2002 Writing with DNA and protein using a nanopipet for controlled delivery *J. Am. Chem. Soc.* **124** 8810–1

[12] Chung S-W, Ginger D S, Morales M W, Zhang Z, Chandrasekhar V, Ratner M A and Mirkin C A 2004 Top-down meets bottom-up: dip-pen nanolithography and DNA-directed assembly of nanoscale electrical circuits *Small* **1** 64–9

[13] Mrksich M and Whitesides G M 1995 Patterning self-assembled monolayers using microcontact printing: a new technology for biosensors? *Trends Biotechnol.* **13** 228–35

[14] Bernard A, Renault J P, Michel B, Bosshard H R and Delamarche E 2000 Microcontact printing of proteins *Adv. Mater.* **12** 1067–70

[15] Wälti C, Wirtz R, Germishuizen W, Bailey D, Pepper M, Middelberg A and Davies A 2003 Direct selective functionalization of nanometer-separated gold electrodes with DNA oligonucleotides *Langmuir* **19** 981–4

[16] Widrig C A, Chung C and Porter M D 1991 The electrochemical desorption of n-alkanethiol monolayers from polycrystalline Au and Ag electrodes *J. Electroanal. Chem. Interfacial Electrochem.* **310** 335–59

[17] Labukas J P and Ferguson G S 2011 Direct route to well-defined, chemically diverse electrode arrays *Langmuir* **27** 3219–23

[18] Lai R Y, Lee S-H, Soh H T, Plaxco K W and Heeger A J 2006 Differential labeling of closely spaced biosensor electrodes via electrochemical lithography *Langmuir* **22** 1932–6

[19] Evans D, Johnson S, Laurenson S, Davies A G, Ferrigno P K and Wälti C 2008 Electrical protein detection in cell lysates using high-density peptide-aptamer microarrays *J. Biol.* **7** 3

[20] Zhu H, Yan J and Revzin A 2008 Catch and release cell sorting: electrochemical desorption of T-cells from antibody-modified microelectrodes *Colloids Surf.* B **64** 260–8

[21] Porath D, Bezryadin A, de Vries S and Dekker C 2000 Direct measurement of electrical transport through DNA molecules *Nature* **403** 635–8

[22] Hwang J S, Kong K J, Ahn D, Lee G S, Ahn D J and Hwang S W 2002 Electrical transport through 60 base pairs of poly(dG)-poly(dC) DNA molecules *Appl. Phys. Lett.* **81** 1134–6

[23] Hashioka S, Saito M, Tamiya E and Matsumura H 2004 Deoxyribonucleic acid sensing device with 40 nm-gap-electrodes fabricated by low-cost conventional techniques *Appl. Phys. Lett.* **85** 687–8

[24] Guo X, Gorodetsky A A, Hone J, Barton J K and Nuckolls C 2008 Conductivity of a single DNA duplex bridging a carbon nanotube gap *Nat. Nanotechnol.* **3** 163–7

[25] Choi Y-K, Lee J S, Zhu J, Somorjai G A, Lee L P and Bokor J 2003 Sublithographic nanofabrication technology for nanocatalysts and DNA chips *J. Vac. Sci. Technol.* B **21** 2951–5

[26] Roy S, Chen X, Li M-H, Peng Y, Anariba F and Gao Z 2009 Mass-produced nanogap sensor arrays for ultrasensitive detection of DNA *J. Am. Chem. Soc.* **131** 12211–7

[27] Peterson A W, Heaton R J and Georgiadis R M 2001 The effect of surface probe density on DNA hybridization *Nucleic Acids Res.* **29** 5163–8

[28] Wirtz R, Wälti C, Germishuizen W A, Pepper M, Middelberg A P J and Davies A G 2003 High-sensitivity colorimetric detection of DNA hybridization on a gold surface with high spatial resolution *Nanotechnology* **14** 7–10

[29] Porter M D, Bright T B, Allara D L and Chidsey C E D 1987 Spontaneously organized molecular assemblies: IV. Structural characterization of n-alkyl thiol monolayers on gold by optical ellipsometry, infrared spectroscopy, and electrochemistry *J. Am. Chem. Soc.* **109** 3559–68

[30] Yau H, Chan H, Sui S and Yang M 2002 Integrity and redox properties of homogeneous and heterogeneous DNA films on gold surface probed by cyclic voltammetry *Thin Solid Films* **413** 218–23

[31] Boozer C, Chen S and Jiang S 2006 Controlling DNA orientation on mixed ssDNA/OEG SAMs *Langmuir* **22** 4694–8

[32] Ishige Y, Shimoda M and Kamahori M 2006 Immobilization of DNA probes onto gold surface and its application to fully electric detection of DNA hybridization using field-effect transistor sensor *Japan. J. Appl. Phys.* **45** 3776–83

[33] Sauthier M L, Carroll R L, Gorman C B and Franzen S 2002 Nanoparticle layers assembled through dna hybridization: characterization and optimization *Langmuir* **18** 1825–30

[34] Keighley S D, Li P, Estrela P and Migliorato P 2008 Optimization of DNA immobilization on gold electrodes for label-free detection by electrochemical impedance spectroscopy *Biosens. Bioelectron.* **23** 1291–7

[35] Steichen M and Buess-Herman C 2005 Electrochemical detection of the immobilization and hybridization of unlabeled linear and hairpin DNA on gold *Electrochem. Commun.* **7** 416–20

[36] Demers L M, Östblom M, Zhang H, Jang N-H, Liedberg B and Mirkin C A 2002 Thermal desorption behavior and binding properties of DNA bases and nucleosides on gold *J. Am. Chem. Soc.* **124** 11248–9